Synthesis and Characterization of Polypyrrole Composites for Corrosion Protection of Steel

M. Selvaraj, S. Palraj, K. Maruthan, G. Rajagopal, G. Venkatachari

Corrosion Science and Engineering Division, Central Electrochemical Research Institute, Karaikudi 630006, India

Received 10 January 2008; accepted 24 October 2008
DOI 10.1002/app.31430
Published online 5 January 2010 in Wiley InterScience (www.interscience.wiley.com).

ABSTRACT: Corrosion protection performance of epoxy polyamide coatings containing polypyrrole (PPy) composites for steel has been studied. PPy and its composites have been synthesized chemically using potassium permanganate and potassium per sulfate as oxidants. The PPy has been characterized by four probe method for conductivity, atomic absorption spectroscopy for elemental analysis, and Fourier transform infrared spectra for proving the incorporation of dopant in this polymers. The X-ray diffraction (XRD) study has revealed the presence of manganese dioxide in the polymer. The elemental analysis and the thermo gravimetric analysis measurements showed that the presence of manganese dioxide in the polymer is about 75%. The thermal stability of deprotonated polymer has improved. Electrochemical impedance spectroscopic analysis indicated that the epoxy polyamide/PPy-MnO_2 coating showed the maximum resistance value of 2.196×10^7 Ω cm^2 after 30 days immersion in 3% sodium chloride solution. © 2010 Wiley Periodicals, Inc. J Appl Polym Sci 116: 1524–1537, 2010

Key words: corrosion resistance; polypyrrole; XRD; elemental analysis

INTRODUCTION

Polymer coatings are most widely used to protect steel structures from corrosive environments.[1,2] In recent years, studies have proven that the conducting polymers are useful to protect the ferrous and nonferrous metals from corrosive atmosphere. Most of the investigations on corrosion studies have been carried out with polyaniline[3–5] and polypyrrole (PPy)[6–9] along with suitable dopant. It is reported that the conducting property and the yield of the polymers are dependent on the nature of the oxidant and surfactant used in the synthesis.[10] Owing to high conductivity and ease of preparation and excellent stability, PPy, is preferred to other conducting polymers for protecting the steel structures from corrosion. In chemical polymerization, the transition metal ions containing compounds are generally used as an oxidizing agent (Fe^{3+}, Cu^{2+}, Cr^{6+}, Ce^{4+}, and Mn^{7+}).[11] The chromium-based oxidant produce toxic chromium compounds during the preparation of PPy and the chromium forms as passive layer over the substrate when PPy is used as a protective coating for ferrous and nonferrous surfaces.[12] To reduce the toxic property, it has been attempted to use potassium permanganate and potassium per sulfate as oxidizing agents to produce PPy. The addition of surfactants is found to accelerate the formation of PPy and also increase the conductivity of the polymer. The thermal resistance and stability of the polymer are also increased by the addition of anionic surfactant as dopant into PPy.[11]

Epoxy polyamide coatings are well-known in protecting steel structures from neutral and marine environments.[13,14] Further, addition of 0.3–1.5% of PPy composite with the epoxy coating formulation has been found to improve the corrosion resistance property.[15] The electrochemically prepared PPy has got very good anticorrosive property, which is equal to the zinc rich coatings.[16] In this study, the PPy composite powder is incorporated in the epoxy polyamide binder and coated on sand blasted steel surfaces. The corrosion protective performance of this coating is evaluated through accelerated salt spray test and electrochemical impedance measurements in 3% sodium chloride solution. The protective ability of the composite coating is discussed in this article.

EXPERIMENTAL

Pyrrole (Acras) was distilled under vacuum and stored in refrigerator before use. The oxidants potassium per sulfate (Qualigen) and potassium per manganate (Qualigen) and the surfactant sodium dodecyl benzene sulfonate (Sigma) were used as

Correspondence to: G. Rajagopal (dhadi.rajagopal@gmail.com).

received. Epoxy resin of bisphenol-A type with epoxy equivalent 450–500 supplied by Ciba Specialty Chemicals, Mumbai and the hardener, polyamide with amine value 210–230 supplied by Synpol Synthetic Polymers Pvt., Ahmadabad were used for this study. Solvent mixed xylene (Qualigen) was also used for adjusting viscosity of the polymer used for coatings.

Synthesis of polypyrrole

PPy was prepared by chemical polymerization in distilled water containing 0.1 mol of potassium per sulfate or potassium permanganate in 150 mL of distilled water in a reaction vessel. Distilled pyrrole (0.05 mol) was dissolved in 50 mL of distilled water and added dropwise to the above solution. The reaction mixture was stirred continuously by a magnetic stirrer. The polymerization was continued for 4 h at room temperature. The PPy was filtered and washed with distilled water and dried in vacuum at 50°C for 8 h.

Preparation of polypyrrole with oxidants and surfactant

In the same way as mentioned earlier, 0.05 mol of potassium persulfate or potassium permanganate was dissolved in 100 mL of distilled water in a reaction vessel. Also 0.01 mol of surfactant (DBSNa) dissolved in 100 mL of distilled water was added to the above reaction vessel and stirred for 15 min using magnetic stirrer. Then, 0.15 mol of distilled pyrrole dissolved in 50 mL of water was added dropwise to the above solution and continued the stirring for 4 h at room temperature. The PPy was washed with distilled water and dried in a vacuum oven at 50°C for 8 h.

Neutralization

The nomenclature of these PPy polymers were given in Table I. A part of the PPy powder prepared was treated with an excess solution of ammonium hydroxide for 12 h. The PPy was filtered and washed with distilled water and dried at 60°C in a vacuum oven.

Preparation of PPy incorporated epoxy-polyamide coating

Epoxy resin was diluted with xylene to 49% solution and added 1 g of PPy to it and grounded well to get 1% PPy incorporated base part for this study. The hardener, polyamide was also modified to get 49% solution using xylene as solvent and incorporated 1 g of PPy in it and grounded well to get 1% PPy hardener solution.

Mild steel panels of 10 cm × 15 cm size were sandblasted to get near white surface profile as per Swedish standard SA 2.5.[17] The base and hardener parts were mixed in the ratio of 70 : 30 and applied over the sand blasted steel surfaces by brush and dried for 15 days. The panels with coating thickness 40 ± 5 μm were selected for corrosion studies. Similarly, a set of panels were coated with the epoxy-polyamide coating and used as control for comparison of results.

Characterization

The PPy compositions were estimated by elemental analysis using atomic absorption spectroscopy of Varian Spectra AA 220, Australia. Dry PPy powder was used to make 1 mm thick, 12.5 mm dia pellets, and its conductivity was measured by four probe method having 1 cm as the distance between the terminals and using a Keithley' 2182 nano voltmeter in conjunction with 2400 source meter. The structural properties of the polymer were determined by Fourier transform infrared (FTIR) spectrum using model Nicolas-670, UK. The grain size of the PPy was studied by X-ray diffraction using X pertPRO PAN analytical diffractometer with Syn Master793s Software.

Thermo gravimetric analysis (TGA) and differential scanning calorimeter (DSC) measurements were carried out in the flow of nitrogen (100 mL m^{-1}) at a heating rate of 10°C m^{-1} using SDT Q600, TA instruments, USA. The DGA and DSC curves were recorded simultaneously.

The surface morphology of the PPy's were studied by scanning electron microscope (SEM) model JOEL, JSM 35F, Japan

Corrosion studies

Accelerated salt spray test

The coated panels in duplicate were scratched at the center and exposed in the salt spray chamber, where 5% sodium chloride solution was atomized by compressed air to create a fog. This test was conducted in accordance with ASTM standard B117 for 500 h.

Electrochemical impedance spectroscopy (EIS)

The corrosion resistance properties of epoxy-polyamide and epoxy polyamide incorporated with 1% PPy coatings on steel surface were evaluated by AC impedance spectroscopy. The impedance measurements were carried out with PAR model 6310 electrochemical impedance analyzer in the frequency range of 10 kHz to 100 MHz and for applied signal amplitude of 20 mV. The electrochemical cell used for this study consists of polymer coated electrode as working electrode, a platinum foil as counter, a

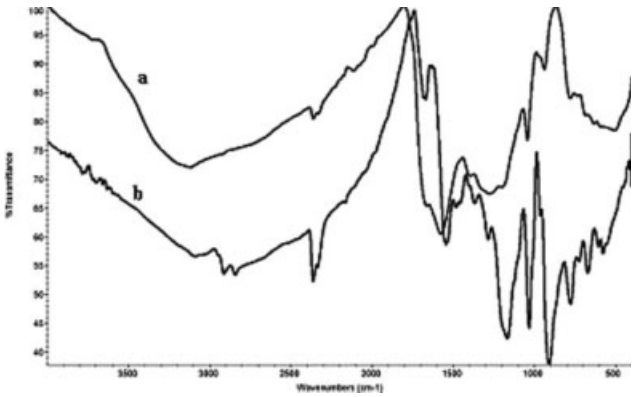

Figure 1 FTIR spectrum of PPy-SO_4 prepared by (a) potassium persulfate as oxidant and (b) oxidant and Na DBSA as surfactant.

saturated calomel electrode as reference electrode, and 3% NaCl solution as the electrolyte. The impedance measurements were carried out periodically for 30 days.

RESULTS AND DISCUSSION

FTIR spectral analysis

FTIR spectra of persulfate oxidized PPy and the surfactant incorporated PPy are shown in the Figure 1. It is observed from the spectra that a broad band observed between 3500 cm^{-1} and 2000 cm^{-1} corresponds to the presence of N—H linkages in the polymer. This is due to the molecular association of PPy with the N—H linkages in the polymer. The band at 1575 cm^{-1} corresponds to the C—C stretching vibration within the pyrrole ring. The bands at 1278 cm^{-1} and 1041 cm^{-1} in the spectrum are attributed to C—H and C—N in-plane deformation mode. The band with sharp peak at 938 cm^{-1} represents the vibrations of C—C bond due to plane deformation. The peak at 779 cm^{-1} with broad band between 700 cm^{-1} and 500 cm^{-1} denotes that the vibrations of C—H and C—C bond with out of plane ring deformation are similar to that of Ping.[18] The broad band between 1000 cm^{-1} and 1300 cm^{-1} with a peak at 1120 cm^{-1} and 600 cm^{-1} indicates the presence of sulfate group in the polymer.

By comparing the spectra 1(a) with 1(b), the PPy prepared in the presence persulfate and anionic surfactant indicate that they are almost similar with the formation of few new peaks and overlapping bonds. The new peak at 1160 cm^{-1} represents the presence of sulfoxide group in the polymer. Further, the broad bands observed between 500 cm^{-1} and 600 cm^{-1} with peaks at 669 cm^{-1} and 604 cm^{-1} denote the presence of sulfate groups in the molecules. The concentration of the sulfonate and sulfoxide groups are expected to be higher than the corresponding spectra 1(a). The other peaks are similar to the 1 (a) spectra with minor shift in the peak values.

FTIR spectra of PPy prepared using potassium permanganate as oxidant and with surfactant are shown in Figure 2. The broad band observed in the region of 3700–2700 cm^{-1} is due to the molecular association of PPy with the N—H linkages. Generally, this type of linkage indicates the presence of —OH and —NH_2 groups in the molecule. But in this

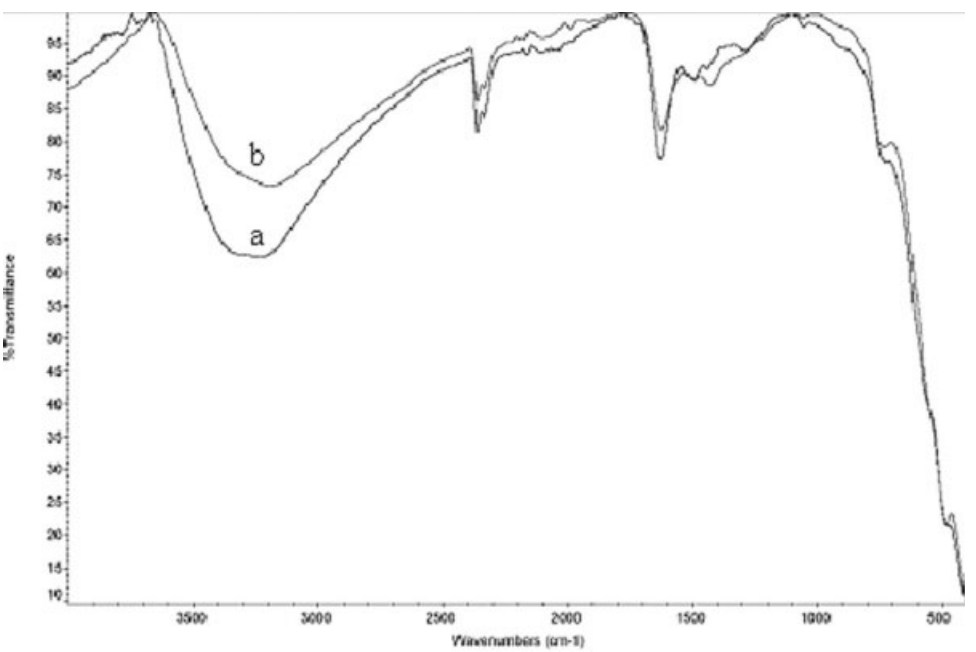

Figure 2 FTIR spectrum of PPy-MnO_4 prepared by (a) potassium permanganate as oxidant and (b) oxidant and Na DBSA as surfactant.

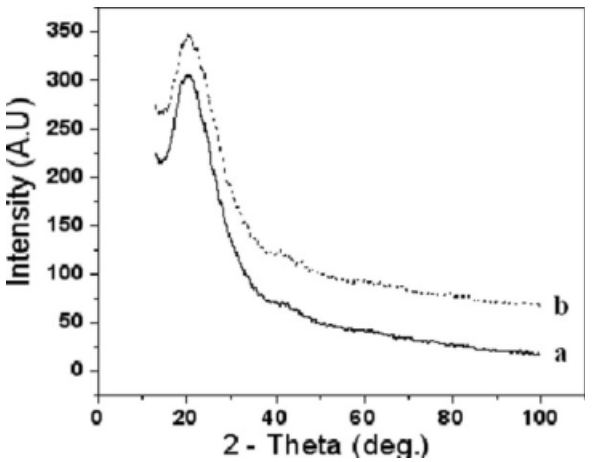

Figure 3 XRD pattern of PPy-S_2O_8 (a) prepared by potassium persulfate as oxidant and (b) the oxidant and SDBS as surfactant.

polymer, there is no possibility of formation of —OH groups. Thus, this peak is mainly due to the PPy associated through N—H linkages. This broad band is depressed in the surfactant incorporated PPy polymer. The significant reflection of this depression is attributed to intrachain excitations.[19]

The peaks observed in the region of 1540–1600 cm^{-1} denotes the presence of C—N linkages in the pyrrole ring. The sharp peaks at 1631 cm^{-1} and 1493 cm^{-1} indicate the C—C bond position of pyrrole molecule. This peak is slightly shifted to lower wave number for surfactant treated polymer and no other significant changes are observed in the spectrum of the polymer. The appearance of MnO_4 group is indicated by the presence of small peak at 700 cm^{-1} and 485 cm^{-1}. These are the characteristic peaks for the manganate group.[20] Further, the appearance of characteristic peaks for sulfoxide group is completely absent in the Figure 2(b). There are no peaks observed at 1160 cm^{-1} and 1030 cm^{-1}, hence the surfactant radicals are not incorporated within the PPy-MnO_4 polymer. Thus, there is no influence of the surfactant in the structure of the polymer. This result is also reflected in the elemental analysis where the percentage of manganese is similar for both the polymers. The conductivity was also very low for these PPy's.

X-ray diffraction analysis

The X-ray diffraction (XRD) pattern for the PPys using the potassium persulfate and the anionic surfactant are shown in the Figure 3. It is observed from the figure that the polymer is in an amorphous state, and hence there are no sharp peaks observed in the diffraction pattern. But a broad peak at about 24° of 2θ value is observed, which incidentally is the characteristics peak of amorphous PPy polymer.[21] XRD pattern of pure amorphous manganese dioxide are indexed and characterized by the small broad peaks at 68° and 38° of 2θ value.[22] Figure 4 presents the XRD pattern of PPy/MnO_2 and also with the surfactant reveals the amorphous state of PPy-MnO_2. The peaks at 38° and 68° of 2θ values are similar to pure amorphous manganese dioxide particles. The appearance of an incomplete broad peak at 20° of 2θ values indicates the presence of PPy as a major component in the composite. Similar diffraction pattern for the PPy-MnO_4-SDBS is observed in the Figure 4. The average particle size of the composite polymer is calculated by using the Scherrer's formula,

$$D = \frac{0.94\lambda}{\beta \cos\theta}$$

where D is size of the particle, $\lambda = 1.5418 \times 10^{-10}$ Å, θ = the cosine of the Bragg angle, and β = the full width at half height of angle of diffraction in radians.

The above equation leads to particle size of the PPy-SO_4 composite polymer sample could be about 100 nm and that of PPy-MnO_4 is in the range of 40–50 nm. Thus, the XRD analysis shows that the PPy particles are smaller in size and also the presence of manganese dioxide in it. There is no appreciable difference in XRD pattern for the surfactant treated PPy.

The FTIR spectroscopy and the XRD studies enable the structural identification of the PPy-SO_4 and of PPy-MnO_4 are as shown in Figure 5. The presence of sulfate group and the N—H stretch is indicated in the corresponding peaks of FTIR spectrum of PPy-SO_4 polymers. Similarly, the presence of manganate and N—H vibration bands strongly influence the

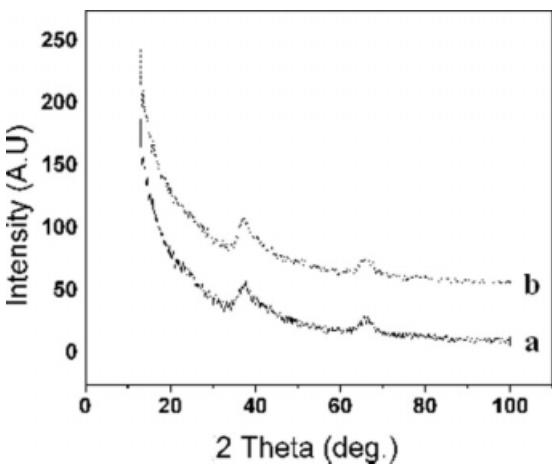

Figure 4 XRD pattern of Ppy-MnO_4 (a) prepared by potassium permanganate as oxidant and (b) the oxidant and SDBS as surfactant.

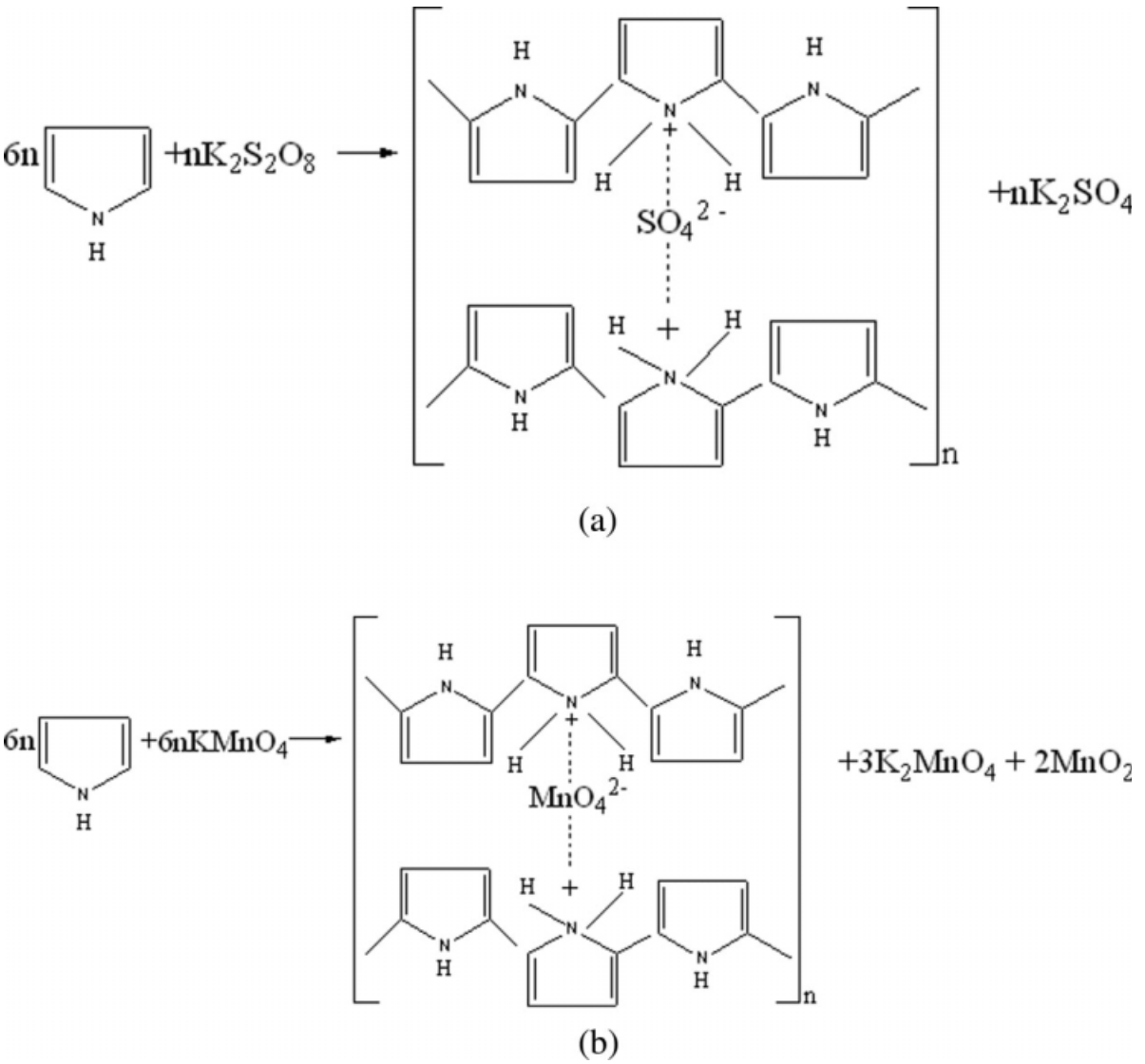

Figure 5 (a and b) Structure of polypyrol prepared by using potassium persulfate and potassium permanganate as oxidant.

PPy-MnO_4 structure. The peak between 1050 cm^{-1} and 1100 cm^{-1} is very sharp for the sample with anionic surfactant of PPy-SO_4. This peak is also present in the PPy-SO_4 with lesser intensity. The presence of this peak is also observed for PPy-MnO_4 composite with minimal intensity. This can be one of the reasons for the higher conductivity of PPy prepared using potassium persulfate than that of PPy prepared by using potassium permanganate. Thus, we suggest that this corresponding peak in plane deformation vibration of N^+H_2, which is formed on the PPy chains by protonation.[23] Generally, this

TABLE I
Nomenclature of the Coating System

No.	Polymers preparation processes	Nomenclature
1	Polypyrrole-potassium persulfate	PPy-SO_4
2	Polypyrrole potassium persulfate oxidant, deprotonated	PPy-SO_4 (dep)
3	Polypyrrole-potassium permanganate oxidant	PPy-MnO_4
4	Polypyrrole-potassium permanganate oxidant deprotonated	PPy-MnO_4 (dep)
5	Polypyrrole-potassium persulfate oxidant and sodium dodecyl benzene sulfonate	PPy-SO_4-SDBS
6	Polypyrrole-potassium persulfate oxidant and sodium dodecyl benzene sulfmate deprotonated	PPy-SO_4-SDBS (dep)
7	Polypyrrole-potassium permanganate oxidant and sodium dodecyl benzene sulfonate	PPy-MnO_4-SDBS
8	Polypyrrole-potassium permanganate, sodium dodecyl base sulfomate deprotonated	PPy-MnO_4-SDBS (dep)

TABLE II
Data for Elemental Analysis and Conductivity of PPy Polymers Prepared under Different Conditions

No.	Polymerization condition	Additive	Elemental compositions (wt %) C	H	N	S	Mn	Conductivity (S cm^{-1})
1	$K_2S_2O_8$ as oxidant	–	48.7	4.02	14.5	1.42	–	3.42×10^{-1}
2	$K_2S_2O_8$ oxidant deprotonated using NH_4OH	–	49.5	4.11	15.5	0.75	–	1.53×10^{-2}
3	$K_2S_2O_8$ as oxidant	NaDBS	61.6	6.04	11.1	3.55	–	3.59×10^{-1}
4	$K_2S_2O_8$ oxidant deprotonated using NH_4OH	NaDBS	60.1	5.93	11.4	2.71	–	7.478×10^{-3}
5	$KMnO_4$ as oxidant	–	34.6	11.2	0.58	–	40.1	5.307×10^{-2}
6	$KMnO_4$ as oxidant and deprotonated by NH_4OH	–	34.5	6.75	2.23	–	35.6	9.478×10^{-3}
7	$KMnO_4$ as oxidant	NaDBS	36.2	14.4	2.62	0.23	22.5	5.13×10^{-2}
8	$KMnO_4$ as oxidant and deprotonated by NH_4OH	NaDBS	41.8	8.71	10.4	0.19	20.2	9.24×10^{-3}

protonated groups have an electron affinity with the SO_4^{2-} groups present in the formation of a bridge structure between the two protonated PPy chains. Hence, the suggested structure of PPy-SO_4 is as in the Figure 5. Similarly, the structure of PPy-MnO_4 is also arrived with very low percentage of such linkages, because this polymer composite contains excess of manganese dioxide present as impurities.

Elemental analysis and conductivity measurements

Table II summarizes the elemental analysis data and the conductivity measurements for PPy polymer prepared under various conditions. It is observed that there is no evidence for the presence of potassium in the PPy-SO_4 and PPy-SO_4-SDBS polymers. The increase in content of manganese is not observed in the PPy polymer prepared with SDBS, but a decreasing tendency is observed. The decrease in the content of manganese for the PPy-MnO_4-SDBS is mainly due to the reaction of the surfactant with the manganese and gets washed away in the distilled water. The manganese content in PPy-MnO_4 is very high with 40.105% and slightly decreased the content after deprotonation. The decrease in manganese in deprotonated PPy-MnO_4 is due to removal of some of the MnO_4^{2-} radicals from the PPy and form soluble manganese salt, which is removed from the polymer composite by distilled water washing. Similar behavior has been observed in the deprotonated PPy-MnO_4-SDBS polymers also.I

The conductivity of the PPy-SO_4 and PPy-SO_4-SDBS is higher than that of other polymers. It is in the range of 0.359–0.342 S cm^{-1}. The increase in conductivity of PPy-SO_4 polymer is mainly due to the formation of high protonated N—H bonds in this polymer than in other PPy systems. The conductivity of PPy-MnO_4 polymer is very low due to the presence of excess manganese dioxide particles along with the polymer. The manganese dioxide hindered the conductivity and it is in the order of 5.307×10^{-2} S cm^{-1} for PPy-MnO_4 and 5.13×10^{-2} S cm^{-1} for PPy-MnO_4-SDBS. This result indicates that there are no significant changes in conductivity of surfactant doped polymers. Hence, it can be concluded that the conductivity of these two polymers are almost identical. Further, the undissociated molecules of the surfactant form thick layer over the PPy surface during the polymerization process and so it may function as steric stabilizer. The presence of this stabilizer leads to considerable decrease in particle size and conductivity of PPy as mentioned by Aldissi and Armes.[24]

Thermo gravimetric analysis

The thermal stability of the PPy prepared in the presence of oxidants and surfactants was studied by TGA. Figure 6 presents the curves of weight loss and temperature differences of PPy-SO_4 and PPy-SO_4-SDBS polymers. The corresponding weight loss data are given in the Table III. The first weight loss has been observed below 100°C for PPy-SO_4 polymer, whereas this weight loss is not observed in PPy-SO_4-SDBS polymer. The first weight loss for PPy-SO_4 is due to the evaporation of water

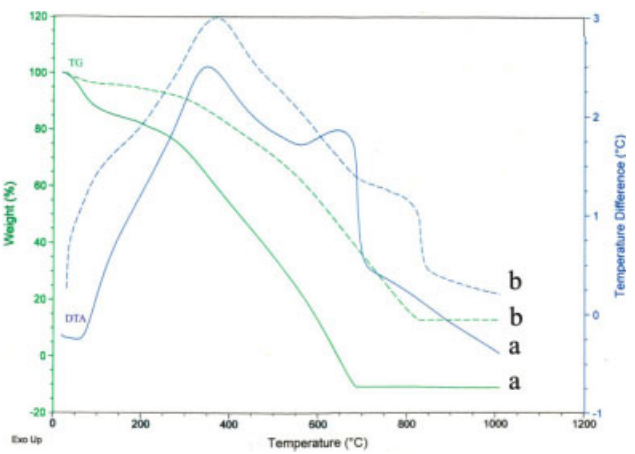

Figure 6 Thermo gravimetric diagram of PPy-SO_4 and PPy SO_4-SDBS polymers. [Color figure can be viewed in the online issue, which is available at www.interscience.wiley.com.]

TABLE III
Weight Loss Data's from TGA Analysis for PPy Polymers Prepared by Different Oxidants and Anionic Surfactant

No.	Weight loss and temperature	PPy-SO_4		PPy SO_4-SDBS		PPy MnO_4		PPy MnO_4 SDBS	
		BN	AN	BN	AN	BN	AN	BN	AN
1	Temperature TG (°C)	40–97	40–95	–	–	–	–	40–173	40–154
	Weight loss	10.71	10.14	–	–	–	–	14.72	18.57
2	Temperature TG (°C)	97–241	95–273	40–292	40–303	40–209	40–207	173–495	154–509
	Weight loss	7.44	8.42	8.75	18–98	16.75	20.44	3.63	4.94
3	Temperature TG (°C)	241–686	273–750	292–827	303–691	207–493	207–493	495–827	509–810
	Weight loss	78.48	76.43	78.18	82.13	4.84	3.85	3.77	5.35
4	Temperature TG (°C)	1000	1000	1000	1000	1000	1000	1000	1000
	Residue	3.028	5.33	13.09	1.979	278.52	76.22	77.56	71.14

BN, before neutralization; AN, after neutralization.

molecules present in the polymer. This weight loss has not been noticed in the surfactant incorporated polymer because the surfactant encapsulates the polymer and the water present in the polymer is negligible. When this negligible amount of water is evaporated, minimum weight loss is observed as in the figure. The second phase of weight loss is observed for PPy-SO_4 with the loss of 7.44% of the polymer. This weight loss is not observed in PPy-SO_4-SDBS polymer. This small weight loss occurs below 260°C is due to the disintegration of impurities present in the polymer. Another reason is the PPy starts to degrade beyond 250°C. This is indicated by the third phase of weight loss in PPy-SO_4 and second phase in PPy-SO_4-SDBS. Thus, in this phase 78% weight loss has been observed for both the PPy. In the fourth phase, complete weight loss is observed at 1000°C with a residue of 3% for PPy-SO_4 and 13% for PPy-SO_4-SDBS. Although the shape of both curves is similar in nature, the PPy-SO_4-SDBS sample seems to be more stable than the PPy-SO_4. The performance of deprotonated PPy also has similar trend of degradation as that of the protonated polymer.

The DTA analysis indicates that the PPy-SO_4 polymer has two stages of exothermic reactions with maximum peaks at 352°C and 660°C. In the first stage, the PPy sulfate absorbs the thermal energy up to 300°C and then liberate as exothermic energy. This indicates that the PPy-SO_4 observe require energy up to 300°C to break the protonated sulfate bond. During the breaking of bond, exothermic reaction occurs and it is indicated in the first stage. In the second stage, the PPy polymers absorb energy up to 550°C and then liberate exothermic energy due to the fragmentation of the polymer. These fractions also decompose to form carbon particles of 3% residue. Similar pattern of reaction is observed for surfactant doped PPy-SO_4 polymer, but the exothermic reaction takes place with the peak at 369°C in the first stage. This is due to the liberation of energy due to the breaking of sulfonate and sulfate bond gives more energy than the PPy-SO_4 polymer. Further, for the surfactant encapsulated polymer, it

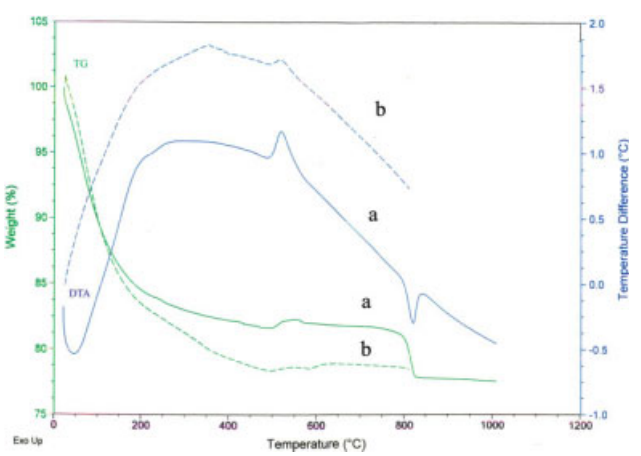

Figure 7 Thermo gravimetric diagram of PPy-MnO_4 and PPy MnO_4-SDBS polymers. [Color figure can be viewed in the online issue, which is available at www.interscience.wiley.com.]

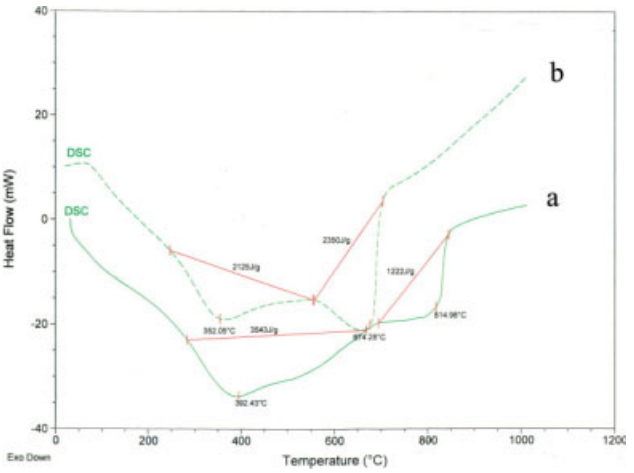

Figure 8 Comparison of DSC spectra for (a) PPy-SO_4 and (b) PPy SO_4-SDBS. [Color figure can be viewed in the online issue, which is available at www.interscience.wiley.com.]

TABLE IV
Characteristic Data Obtained from DSC of PPy Prepared by Using Different Oxidants Anionic Surfactant

No.	Characteristic points	PPy-SO_4		$PPySO_4$-SDBS		PPy MnO_4		PPy MnO_4 SDBS	
		BN	AN	BN	AN	BN	AN	BN	AN
1	Glass transition temperature T_g (°C)	≅70	≅75	≅40	≅50	≅40	≅40	≅50	≅40
2	Reaction (i)								
	(a) Starting temperature (°C)	220	275	275	225	450	460	480	480
	(b) Reaction peak temperature (°C)	352.05	365.65	392.43	346.78	519.99	488.60	518.85	524.04
	(c) Heat of reaction ΔH (J/g)	2120	1128	3543	1395	206.3	255.3	156.3	132.6
3	Reaction (ii)								
	(a) Starting temperature (°C)	550	575	700	550	–	–	800	780
	(b) Reaction peak temperature (°C)	673.78	706.98	814.98	696.42	–	–	818.72	800
	(c) Heat of reaction ΔH (J/g)	2352	2648	1222	1191.7	–	–	109.7	52.84

BN, before neutralization; AN, after neutralization.

requires more energy to break the capsule and so the exothermic reaction starts at 350°C. Another small exothermic reaction occurred between 684°C and 842°C. This is due to the complete disintegration of the polymer with the liberation of energy.

Figure 7 compares the TG and DTA behavior of PPy-MnO_4 and PPy-MnO_4-SDBS samples and the corresponding data are given in the Table III. It is observed that there was no significant weight loss in the first stage below 100°C. The weight loss starts increasing significantly from 200°C with the mass loss of nearly 15% has been observed for both the polymers. This weight loss is mainly due to the loss of moisture and small unreacted monomer present in the polymer. The second phase of weight loss completed in the temperature range of 206–500°C for both the systems with the loss of 3–5% of polymer. This indicates that the PPy present in the composite is decomposed to form small fraction. These fractions also completely eliminated from the polymer composite at 827°C with the residue of 78%. This stable residue has been identified by the XRD as manganese dioxide. From the table, it is found that the deprotonated PPy-MnO_4 and PPy-MnO_4-SDBS also performed in a similar way to protonated polymers with slight decreases in percentage in residue.

The DTA analysis indicates that there are some exothermic reactions and another endothermic reaction peak has occurred in PPy-MnO_4. In the case of PPy-MnO_4-SDBS polymer, a broad exothermic reaction peak with maximum at 580°C has been observed. In the first phase, the PPy-MnO_4 observed energy up to 500°C to break the protonated bond of MnO_4 and then liberate less energy. This quantum of exothermic energy is very low compared with that of PPy-SO_4. This indicates that the energy released due to the breaking of PPy-SO_4 linkage is much higher than that of PPy-MnO_4. The second endothermic reaction is the associated thermal effect due to the cluster formation of manganese dioxide. This association of manganese dioxide is not observed in the case of PPy-MnO_4-SDBS thermogram. This may be due to the presence of sulfonate groups in the surfactant are not allowed the formation of manganese dioxide association. The DTA behavior of deprotonated PPy-MnO_4 and PPy-MnO_4-SDBS polymer is also similar with a small increase in exothermic peaks. This small increase in the exothermic reaction temperature is mainly due to the breaking of the deprotonated polymer bond, which requires more energy than the protonated molecular bonds of PPy.

Differential scanning calorimetric analysis

The DSC Exodown thermogram of PPy-SO_4 and PPy-SO_4 SDBS are shown in Figure 8 and the corresponding reaction data are given in the Table IV. It is observed that the glass transition temperature (T_g) for PPy-SO_4 is 70°C and PPy-SO_4-SDBS is 40°C. The corresponding deprotonated samples also exerted

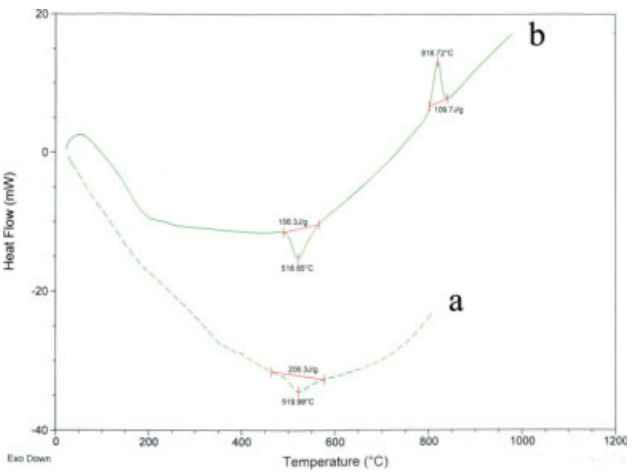

Figure 9 Comparison of DSC spectra for (a) PPy-MnO_4 and (b) PPy MnO_4-SDBS. [Color figure can be viewed in the online issue, which is available at www.interscience.wiley.com.]

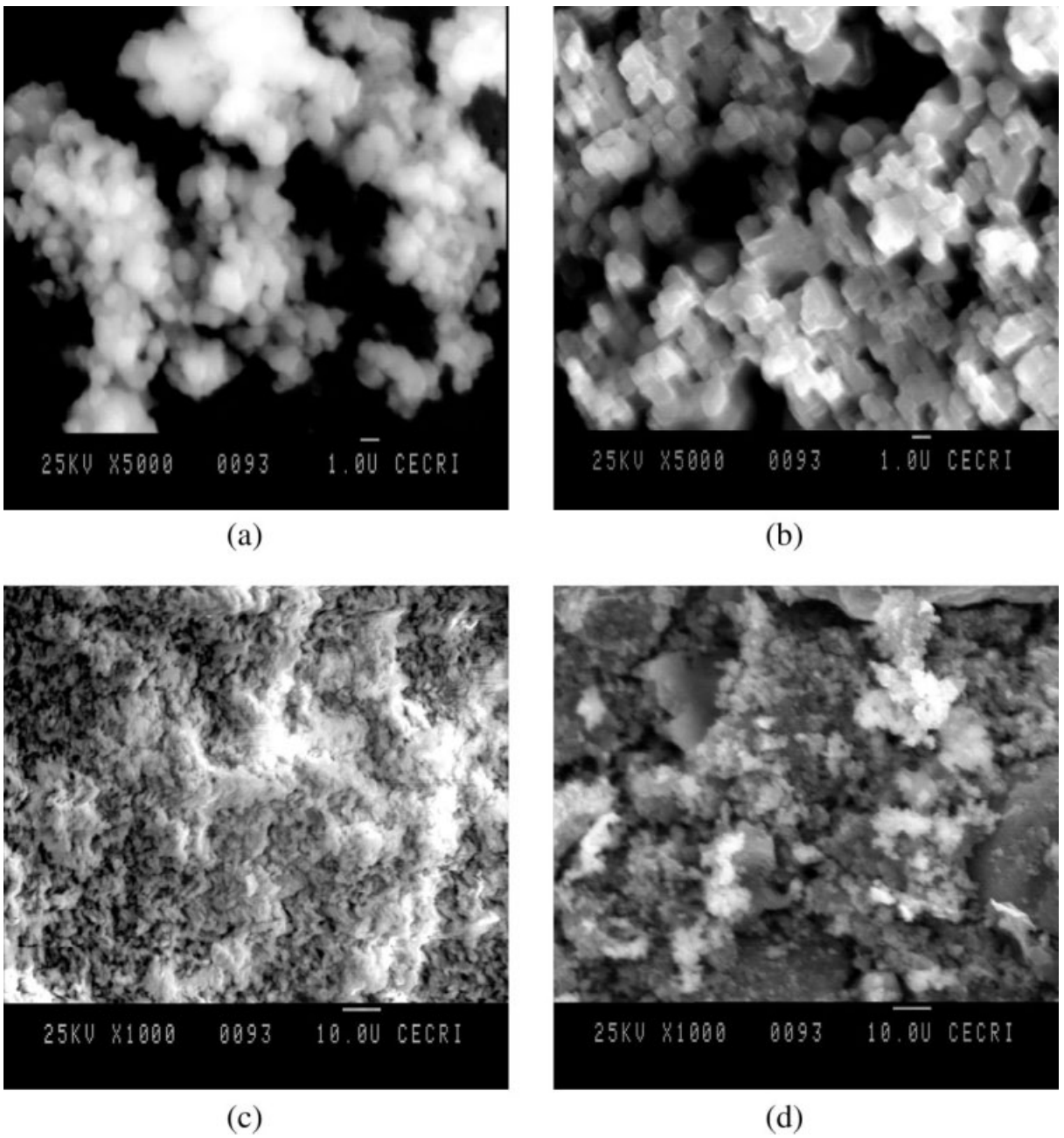

Figure 10 SEM micrograph of (a) PPy-SO_4 without surfactant, (b) deprotonated and PPy prepared in the presence of surfactant, (c) NaDBS, and (d) deprotonated.

similar T_g values at 75°C and 50°C, respectively. The higher T_g value for PPy-SO_4 indicates that the stability of this polymer in the initial stage is better than the surfactant doped polymer. This is due to the stability of sulfonate groups present in the PPy-SO_4-SDBS polymer in the initial stage only. The degradation reaction start at about 220–275°C for all these systems and has the maximum value between 350°C and 390°C. During the reaction, pyrrole ring present in the polymer is broken down to form linear polymer chain with the liberation of 2125 J/g of energy for PPy-SO_4 polymer and 3543 J/g for PPy-SO_4-SBDS polymer.[25,26] At the same time, the corresponding deprotonated polymers liberate the energy in the order of 1128 J/g and 1395 J/g. This result shows that the protonated polymers liberate energy for the breaking of the conducting groups and also the breaking for the cyclic ring. The second stage of reaction is taking place at 550°C for PPy-SO_4 and 700°C for PPy-SO_4-SDBS with the liberation of 2350 J/g and 1222 J/g of energy, respectively. Thus, at the time of disintegration of linear polymer chain of pyrrole releases higher energy level for PPy-SO_4 than the surfactant doped polymer. Thus, the sums

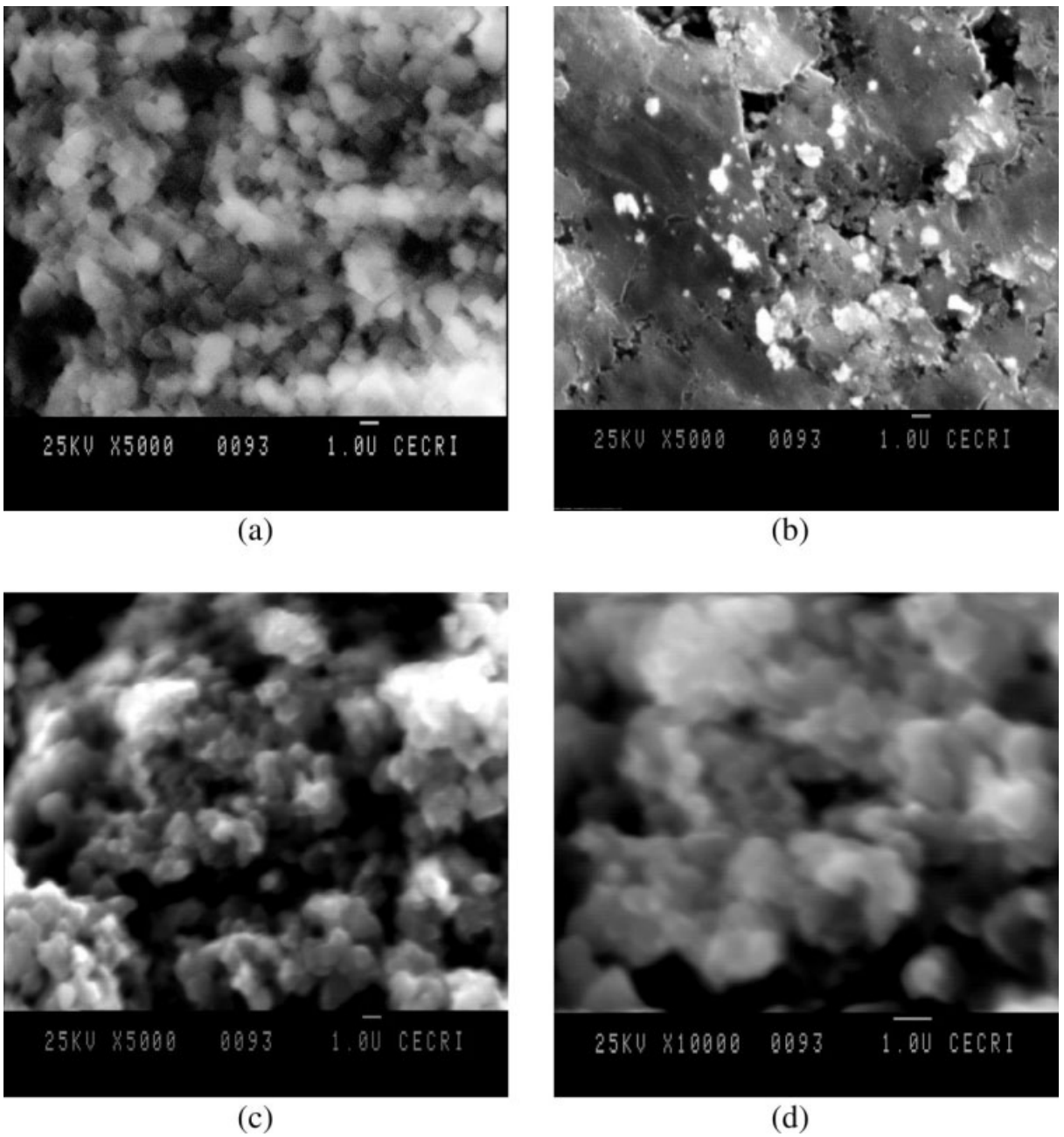

Figure 11 SEM micrograph of (a) PPy-MnO_4, (b) deprotonated and PPy prepared in the presence of surfactant, (c) NaDBS, and (d) deprotonated.

of the two exothermic reactions, the liberated energy level of the two polymers are nearly equal. This result indicates that the total energy liberated by these polymers are same because the chemical reaction takes place in two steps with the opening of cyclic structures in the first stage and the breaking down of the linear polymer as the second stage.

The DSC Exodown thermograms of PPy-MnO_4 and PPy-MnO_4-SDBS are shown in Figure 9 and the corresponding reaction values are given in the Table IV. It is observed that the T_g of these polymers change at 40°C. This indicates that the polymers have slight change in the initial stage, which is due to the liberation of water molecules present in the composite polymer. The dissociation of PPy-MnO_4 takes place in one step, unlike the surfactant doped polymer. The dissociation of PPy-MnO_4 molecule start from 100°C, but the exothermic reaction peak occurs between 450°C and 600°C with the liberation of 206.3 J/g energy. The liberation of this energy is mainly due to the presence of PPy in this polymer which is nearly 22%. The remaining 78% is manganese dioxide. This has been already confirmed in the TGA method. Thus, unlike PPy-SO_4, the PPy-MnO_4

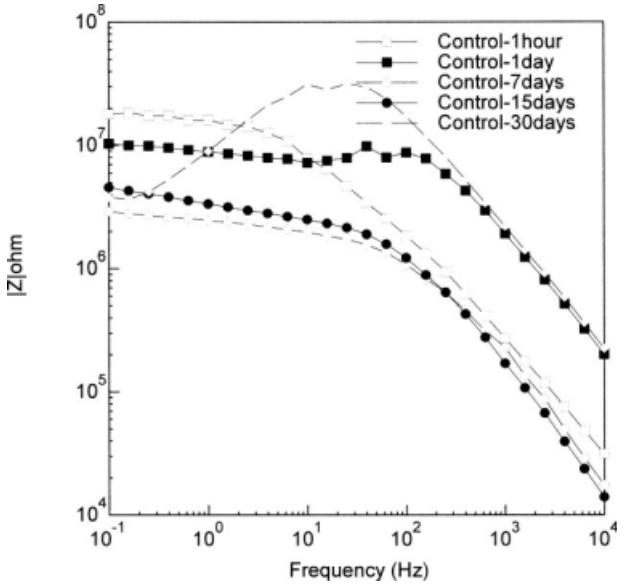

Figure 12 Bode plots of epoxy-polyamide coated mild steel in 3% NaCl solution for different duration.

contains low percentage of PPy polymer and liberates lesser energy during the dissociation. Similar result is also observed for deprotonated PPy-MnO_4 polymers. It has been noticed for the PPy-MnO_4-SDBS polymer, the first exothermic reaction with the liberation of 156.3 J/g energy followed by the endothermic reaction with absorption of 109.7 J/g of energy. Similar performance of deprotonated PPy-MnO_4-SDBS is also observed with slightly lesser value of energy liberation and absorption. This result indicates that in the first stage the PPy dissociates to liberate energy with the formation of manganese dioxide. In the second stage, some association of manganese dioxide molecules takes place with the absorption of energy. This reaction is also indicated in the DTA results.

SEM analysis

As shown in Figure 10, the SEM of PPy-SO_4 exhibits a regular globular structure [Fig. 10(a)]. The structure does not change significantly after doping with SDBS [Fig. 10(b)]. The deprotonated PPy-SO_4 structure [Fig. 10(c,d)] indicates that the structure changed in to clusters and become less porous than the protonated PPy polymer. This structure variation is due to repulsion of the protonated structure of the polymer networks by the presence of proton charges and exhibit as separated globular structure. During the process of deprotonation, the charges disappear and form clusters and the pores present within the network are minimized or disappeared.

The SEM micrographs of PPy-MnO_4 and PPy MnO_4-SDBS are shown in Figure 11. It is seen from Figure 11(a) that the globular structure of PPy is completely eliminated and form scattered uniform granular structure. The structure does not alter much even after doping with SDBS. The magnified structure of PPy-MnO_4-SDBS [Fig. 11(c)] indicates that it is closely packed with PPy and MnO_4 particles in the composite polymer. The deprotonated PPy structure [Fig. 11(b,d)] indicates the appearance

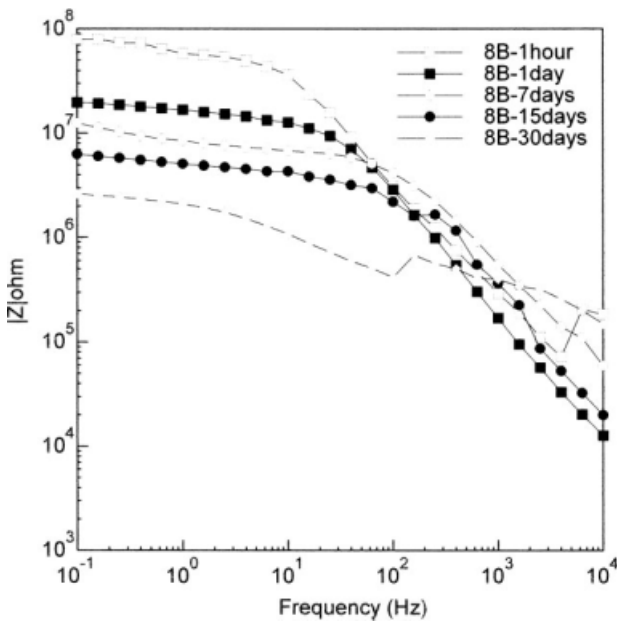

Figure 13 Bode plots of epoxy-polyamide-PPySO_4 incorporated coating on mild steel in 3% NaCl solution for different duration.

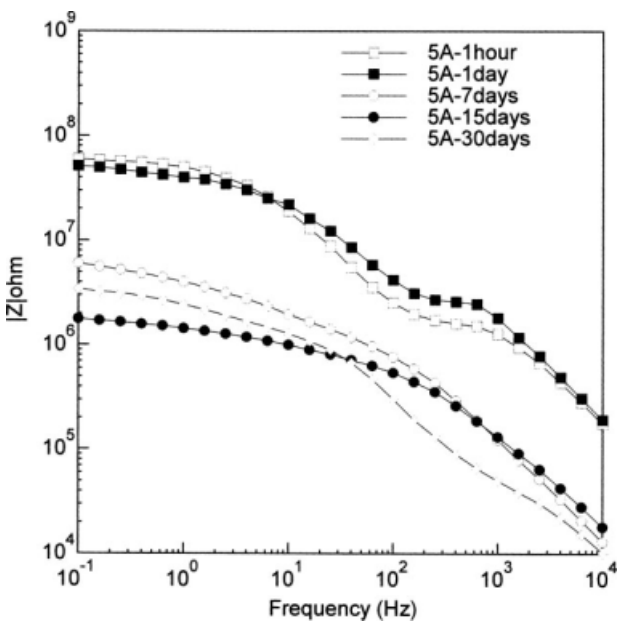

Figure 14 Bode plots of epoxy-polyamide-PPy SO_4 SDBS incorporated coating on mild steel in 3% NaCl solution for different duration.

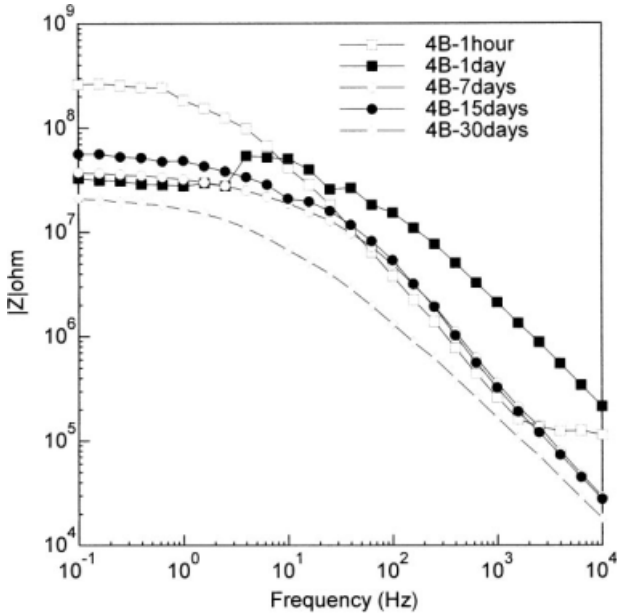

Figure 15 Bode plots of epoxy-polyamide-PPy MnO_4 incorporated coating on mild steel substrate in 3% NaCl solution for different duration.

of globular PPy, which is due to the presence of manganese metal in the composite, is dissolved in ammonia at the time of neutralization.[27] Thus, the manganese dioxide present in the PPy is leached out and, hence, the characteristic globular structure of PPy has been observed after deprotonation. The decrease in manganese content of deprotonated polymer is also confirmed by the elemental analysis.

Corrosion resistance studies

Salt spray test

Periodical observation of PPy incorporated coated panels and the control epoxy polyamide indicates that no corrosion products are seen on the surface up to 240 h of exposure. After 360 h of exposure, corrosion products are seen on the scratched areas of the panels, but there is no spreading of rust beneath the coating. The performance of the coatings in salt spray chamber after 480 h indicate that the protonated PPy polymer incorporated coating exhibit a better protection than deprotonated PPy incorporated coatings. Further, PPy-SO_4-SDBS and PPy-MnO_4-SDBS coated panels have less corrosion resistance than their corresponding protonated composites incorporated coatings. Corrosion products are seen along the scratches, which spread under the coating for PPy prepared in presence of surfactant. The performances of PPy-SO4 and PPy-MnO4 incorporated coatings are in between that of the control epoxy polyamide resin coated panels. Thus, the salt spray test concludes that the PPy-MnO_4 polymer incorporated coatings are highly resistant to corrosive sodium chloride environment than the other systems.

A.C. impedance studies

Electrochemical impedance spectroscopy is used to measure the performance of coating. Figures 12–16 show the Bode plots of control epoxy polyamide and different percentage of PPy incorporated coatings on steel surface for various exposure times in 3% NaCl solution. The capacitance and resistance values exerted by the coatings are given in Table V. The low frequency region indicates the reaction between the interface of metal and polymer layer. It is seen that the charge transfer resistance values decrease with time duration for the control system. Similar behavior has also been observed for all the PPy incorporated systems, but the resistance is high (2.19×10^7 Ω cm^2) for PPy-MnO_4 incorporated coatings after 30 days of exposure. For the same duration, the control system has exerted the resistance of 3.21×10^6 Ω cm^2. Thus, the high resistance values for PPy-MnO_4 can be explained by the effective barrier property of the polymer film. After 30 days of exposure, the resistance exerted by PPy-SO_4 incorporated coating is 3.627×10^6 Ω cm^2 and has the capacitance value 7.2×10^{-10} F cm^{-2}. This indicates that the coating has good barrier protection to the substrate with decrease in water and electrolyte uptake into the coating. The corresponding deprotonated PPy-SO_4 and PPy-MnO_4 shows a low resistance than for the protonated coatings. This is mainly due to the presence of conducting anions in the

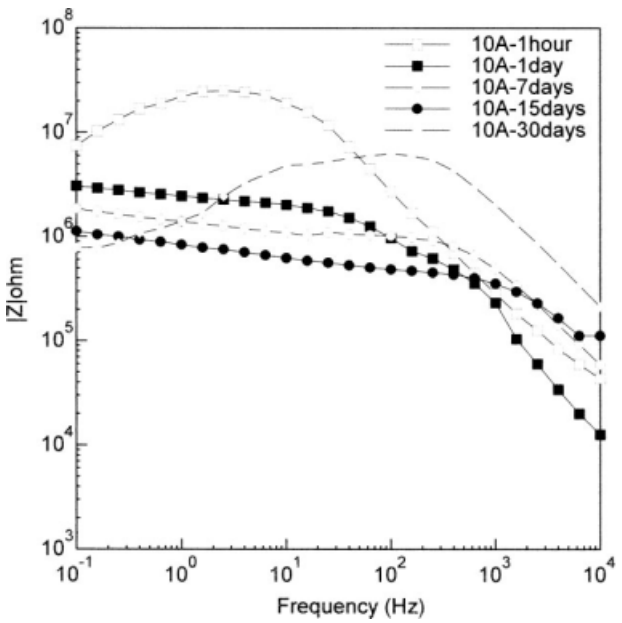

Figure 16 Bode plots of epoxy-polyamide-PPy MnO_4-SDBS incorporated coating on mild steel substrate in 3% NaCl solution for different duration.

TABLE V
Resistance and Capacitance Values Derived from the Bode Plots of PPy-SO_4, PPy-MnO_4 Incorporated Epoxy Coating on Mild Steel Substrate in 3% NaCl Solution

		Resistance (Ω cm^2)		Capacitance (F cm^2)	
Coating system	Duration	Protonated	Deprotonated	Protonated	Deprotonated
Epoxy polyamide	1 h	1.8429×10^7	–	1.2849×10^{-11}	–
	1 day	7.478×10^6	–	$8.9697 \times 10^{-11+}$	–
	7 days	2.355×10^6	–	9.6308×10^{-10}	–
	15 days	3.0058×10^6	–	1.0445×10^{-10}	–
	30 days	3.2157×10^6	–	7.8728×10^{-9}	–
PPy SO_4	1 h	5.34095×10^7	1.9955×10^7	4.6958×10^{-11}	2.51627×10^{-11}
	1 day	1.3556×10^7	2.9766×10^6	5.1346×10^{-11}	7.4331×10^{-10}
	7 days	7.1471×10^6	1.84142×10^6	2.8718×10^{-11}	5.8923×10^{-10}
	15 days	4.6707×10^6	1.6429×10^6	6.0217×10^{-10}	1.3813×10^{-10}
	30 days	3.6272×10^6	2.2926×10^6	7.2402×10^{-10}	2.0611×10^{-10}
PPy SO_4 SDBS	1 h	1.0648×10^8	4.0139×10^7	3.7450×10^{-10}	9.7732×10^{-10}
	1 day	4.4837×10^7	3.1022×10^7	6.2837×10^{-10}	5.0338×10^{-10}
	7 days	7.2091×10^6	9.3738×10^6	8.18257×10^{-9}	1.9367×10^{-10}
	15 days	1.8204×10^6	4.7904×10^6	2.4253×10^{-9}	5.1422×10^{-9}
	30 days	2.9304×10^6	8.5318×10^5	2.1209×10^{-9}	5.9440×10^{-9}
PPy MnO_4	1 h	5.7453×10^8	9.4730×10^7	4.1366×10^{-9}	4.1213×10^{-11}
	1 day	2.8897×10^7	1.9248×10^7	8.4687×10^{-11}	1.1940×10^{-11}
	7 days	4.0105×10^7	1.3131×10^7	5.5491×10^{-10}	2.8145×10^{-10}
	15 days	2.7214×10^7	1.2135×10^7	3.6507×10^{-10}	3.6102×10^{-10}
	30 days	2.1969×10^7	8.2651×10^6	2.5125×10^{-10}	6.7516×10^{-10}
PPy MnO_4 SDBS	1 h	2.4548×10^7	2.3321×10^7	8.6362×10^{-11}	6.2585×10^{-10}
	1 day	2.3864×10^6	1.6332×10^7	6.320010^{-10}	1.6142×1010^{-10}
	7 days	3.31041×10^6	8.7341×10^6	1.4501×10^{-10}	1.6251×10^{-10}
	15 days	6.3323×10^6	1.9624×10^6	8.6362×10^{-11}	3.4609×10^{-10}
	30 days	5.6815×10^6	2.1678×10^5	7.7624×10^{-11}	5.5755×10^{-9}

protonated coating, which are released from the PPy coating and, therefore, the conductivity decreases with time, whereas the barrier properties are increased.[28,29] On the other hand this conductive behavior is not seen in the deprotonated PPy coatings and the deprotonated PPy incorporated coatings exerted low resistance values than the protonated PPy incorporated coatings.

The Figures 14 and 16 show the EIS behavior of PPy-SO_4-SDBS and PPy-MnO_4-SDBS incorporated epoxy coatings after exposures in 3% NaCl and the respective parameters are given in the Table V. The resistance values exerted by these systems after 30 days indicate that it is in higher order of 10^6 Ω cm^2. This shows the higher protection of PPy-MnO_4-SDBS system than the PPy-SO_4-SDBS system. This is due to passivation of iron by MnO_2. This passive oxide film composite prevents corrosion through isolation of charge transfer mechanism. Further, the diffusion of the chloride ions may be restricted by the presence of polyvalent manganese ions.

CONCLUSIONS

Conductive and corrosion inhibitive PPy composites have been synthesized using persulfate and permanganate as oxidants. The FTIR spectra of these samples proved that the anionic surfactant were not doped with the PPy-MnO_4 polymer, but the presence of sulfonate radical in the PPy-SO_4 polymer was indicated. The results of elemental analysis and the TGA indicate that the PPy-MnO_4 polymer contain manganese dioxide to the extent of 78%. The presence of manganese dioxide is responsible for the passivation of steel surface. The XRD data indicate the presence of manganese dioxide in PPy-MnO_4 polymers with particle size between 40 nm and 50 nm. Deprotonated PPy has shown good stability over the protonated polymer but has got poor corrosion protection in 3% sodium chloride solution. The conductivity of PPy-SO_4 and PPy-SO_4-SDBS are in higher order than the PPy-MnO_4 polymer due to the presence of excess manganese dioxide in the polymer composite. The EIS study has shown that the epoxy polyamide/PPy-MnO_4 composite film has exerted high resistance of 2.1969×10^7 Ω cm^2 after 30 days of immersion in 3% sodium chloride solution. At the same time, the control panels showed a resistance of 3.2157×10^6 Ω cm^2. These results have shown that epoxy polyamide with PPy-MnO_4 composite coating has exhibited a better corrosion resistance for the protection of steel surfaces.

References

1. May, C. A.; Tanaka, Y. Epoxy Resin; Marcel Dekker: New York, 1973.

2. Holme, I. Surf Coat Int B Coat Trans 2006, 89, 343.
3. Bernard, M. C.; Joiret, S.; Hugot-Le Goft, A.; Viet Phong, P. J Electrochem Soc 2001, 148, B12.
4. Troch-Nagles, G.; Winard, R.; Wevmeersch, A.; Renard, L. J Appl Electrochem 1992, 22, 752.
5. Syed Azim, S.; Sathiyanarayanan, S.; Venkatachari, G. Prog Org Coat 2006, 56, 154.
6. Atch, D. D.; Navsaria, H. A.; Vadyama, P. J R Soc Interface 2006, 3, 741.
7. Nguyen Thile, M.; Bernard, M. C.; Garcia-Renaud, B.; Deslouis, C. Synth Met 2004, 140, 287.
8. Hosseini, M. G.; Sabouri, M.; Shahrabi, T. Prog Org Coat 2007, 60, 178.
9. Son, A. J. R.; Lee, H.; Moon, B. Synth Met 2007, 157, 597.
10. Hosseini, M. G.; Shahrabi, T.; Sabouri, M. Mater Corros 2006, 57, 407.
11. Kudoh, Y. Synth Met 1996, 79, 17.
12. Twite, R. L.; Bierwagen, G. P. Prog Org Coat 1998, 33, 91.
13. Undrum, H.; Jotun, A. S. J Protective Coat Lining 2006, 23, 52.
14. Selvaraj, M.; Natesan, M.; Jayakrishnan, P. Surface Coat Int B Coat Trans 2002, 85, 229.
15. Armelin, E.; Pla, R.; Liesa, F.; Ramis, X.; Iribarren, J. I. Corros Sci 2008, 50, 721.
16. Rahman, S. U.; Hamayel, M. A. A.; Aleem, B. I. A. Surface Coat Technol 2006, 200, 2948.
17. Venison, J. R. Structural Steel Painting: The International Decorative Paints; Allen Davies and Co. Ltd.: Bristol, England, 1973; pp 5–6.
18. Ping, Z. J Chem Soc Faraday Trans 1996, 92, 3036.
19. Christensen, P. A.; Hammet, A. Electrochim Acta 1991, 36, 1263.
20. Dominak, I. Inorganic Library of FTIR Spectra, Inorganic III, Vol. 3; Nicodom, Nicolet Instruments of Discovery: Prague, Czech Republic, 1998.
21. Pertch, R. E.; Gangoli, S. G.; Matijevic, E.; Cai, W.; Arajs, S. J Colloid Interface Sci 1991, 27, 744.
22. Xu, J. J.; Jain, G.; Yang, J. S. Electrochem Solid State Lett 2002, 5, A152.
23. Omastova, M.; Trchova, M.; Kovarova, J.; Stejskal, J. Synth Met 2003, 138, 447.
24. Aldissi, M.; Armes, S. P. Prog Org Coat 1991, 19, 21.
25. Gundr, Y.; Toppare, L.; Hepuzer, Y.; Yagci, Y. Eur Polym J 2004, 40, 1799.
26. Vishnuvardhan, J. K.; Kulkarni, V. R.; Basavaraja, C.; Raghavendra, S. C. Bull Mater Sci 2006, 29, 7783.
27. Yang, C.; Chen, C. Synth Met 2005, 153, 135.
28. Grgur, B. N.; Krstajie, N. V.; Vojnovic, M. V.; Lacnjevac, C.; Gajic-Krstajic, Lj. Prog Org Coat 1998, 33, 1.
29. Hosseini, H. G.; Sabouri, M.; Shahrabi, T. Prog Org Coat 2007, 60, 178.